Astron. Astrophys. 347, 243–248 (1999)

ASTRONOMY AND ASTROPHYSICS

Acoustic wave energy fluxes for late-type stars

II. Nonsolar metallicities

P. Ulmschneider[1], **J. Theurer**[1], **Z.E. Musielak**[2,3,1], **and R. Kurucz**[4]

[1] Institut für Theoretische Astrophysik der Universität Heidelberg, Tiergartenstrasse 15, D-69121 Heidelberg, Germany
[2] Center for Space Plasma, Aeronomy, and Astrophysics Research, University of Alabama, Huntsville, AL 35899, USA
[3] Physics Department, University of Texas at Arlington, Arlington, TX 76019, USA
[4] Harvard-Smithsonian Center for Astrophysics, 60 Garden St., Cambridge, MA 02138, USA

Received 17 November 1998 / Accepted 16 April 1999

Abstract. Using the Lighthill-Stein theory with modifications described by Musielak et al. (1994), the acoustic wave energy fluxes were computed for late-type stars with the solar metal abundance (population I stars) by Ulmschneider et al. (1996). We now extend these computations to stars with considerably lower metal content (population II stars with 1/10 to 1/1000 of solar metallicity) and find that the acoustic fluxes calculated for stars of different spectral types and different luminosities are affected differently by the metallicity. It is found that the Hertzsprung-Russel diagram can be subdivided into three domains (labeled I, II and III) representing a different dependence of the generated acoustic fluxes on the stellar metal abundance. For the high $T_{\rm eff}$ stars of domain I there is no dependence of the generated acoustic fluxes on metallicity. In domain III are stars with low $T_{\rm eff}$. Here the generated acoustic fluxes are lowered roughly by an order of magnitude for every decrease of the metal content by an order of magnitude. Finally, domain II represents the transition between the other two domains and the generated acoustic fluxes strongly depend on $T_{\rm eff}$. The boundaries between the domains I and II, and II and III can be defined by simple relationships between stellar effective temperatures and gravities.

Key words: convection – hydrodynamics – turbulence – waves – stars: chromospheres – stars: Hertzsprung–Russel (HR) and C-M diagrams

1. Introduction

In our previous work the Lighthill-Stein theory of sound generation has been used to calculate the acoustic wave energy fluxes for population I stars (Ulmschneider et al. 1996, henceforth called Paper I; see also Theurer et al. 1996). To complete the revision of the acoustic wave energy generation in stars with different metallicity, we now extend our previous work to population II stars. To achieve this goal, the opacities used in the stellar envelope models have to be chosen appropriately. In recent years there have been many efforts, e.g. the OPAL and OP projects, to compute absorption coefficients and related variables for a wide range of temperatures, densities and chemical compositions. Despite these efforts, the published opacity tables are still limited in range, especially at low temperatures and densities, where there are numerous contributions by ionizing metals and where molecule formation makes the calculation of the absorption coefficients very difficult. The term 'opacity' is used in the present work to denote the frequency averaged Rosseland mean mass absorption coefficient $\kappa_{\rm Ros}$ (cm^2 g^{-1}), used in the grey radiation treatment of the convection zone code.

The theory of sound generation by turbulence goes back to Lighthill (1952), who was first to develop a method to compute the sound generation from small turbulent flow fields and to apply this theory to solve the problem of jet noise. The famous dependence of sound generation on the eighth power of the turbulent velocity found by Lighthill turned out to be in excellent agreement with terrestrial experiments (e.g., Goldstein 1976). Proudman (1952) subsequently applied Lighthill's theory to the case of homogeneous, isotropic turbulence characterized by Heisenberg's turbulent energy spectrum, and derived a general formula for the generated acoustic power output. Stein (1967) modified the Lighthill-Proudman theory to be more applicable to realistic physical conditions occuring in stellar convection zones. The so-called Lighthill-Stein theory has been modified by Musielak et al. (1994) who incorporated a physically meaningful description of the spatial and temporal spectrum of the turbulent convection. This modified theory was the basis for our computations described in Paper I and will be also adopted here to calculate the acoustic wave energy fluxes for stars of different metallicity.

Since the efficiency of sound generation depends on the eighth power of the turbulent velocity, the maximum acoustic flux is generated in the regions of stellar convection zones where the largest turbulent velocities occur. According to the results obtained in Paper I, there is a narrow region at the top of stellar convection zones where most acoustic wave energy is generated. In stellar convection zones a large part of the total stellar

Send offprint requests to: P. Ulmschneider
Correspondence to: ulmschneider@ita.uni-heidelberg.de

energy flux $F_{\rm tot} = \sigma T_{\rm eff}^4$ is carried by the convective flux. As a given convective flux in a high density region is carried by small flow velocities, it must be transported with large flow velocities in a low density area. Thus, it is clear that large velocities occur at the outer boundary region of the convection zone, where the density is low. By its opacity, this narrow subphotospheric layer of relatively low temperature and density critically determines the maximum of the convective velocity and the decrease of this velocity to much smaller overshoot velocities in the outer radiative equilibrium layer of the photosphere. Adding opacity to a given stellar layer makes it more difficult to transport an appreciable fraction of the total flux by radiation. Hence, the convective flux extends to regions of lower density which leads to larger velocities and to more acoustic flux. As lowering the metallicity decreases the opacity, it thus will lead to lower acoustic flux.

The stellar populations differ in their content of metals. Metals here mean all chemical elements except hydrogen and helium. Population I stars like the Sun have a high metal abundance, while population II stars have 1/10 to 1/100, sometimes even 1/1000 of the solar metal abundance. Obviously, metallicity will influence the efficiency of acoustic wave generation in stars of various spectral types in different ways. Stars, which are hot enough to have the onset of convection in the regions where hydrogen ionization starts, are dominated by hydrogen opacity and they will not be subject to noticeable changes of their acoustic flux even if their metal content is changed. The effects of metallicity will thus be visible primarily in cool stars, where the metal content greatly affects the opacity. Hence, to calculate the acoustic wave energy fluxes generated in stars of different metallicity and various spectral types, opacity tables extending to low temperatures and small densities are required. The opacity tables used in this paper are described in Sect. 2. The calculated stellar acoustic wave energy fluxes and spectra are presented and discussed in Sect. 3. Final conclusions are given in the last section of this paper.

2. Method of computation and opacity tables

For our convection zone computations of late-type stars with different metallicities, we use a standard stellar envelope program that is based on the mixing-length formalism and was described in Paper I. Since the dependence of the generated wave energy fluxes on the mixing-length parameter, α, was extensively discussed in Paper I, and since the results presented there seemed to indicate that $\alpha = 2$ should be used in the wave energy calculations, we adopt here this value for all our calculations. We consider stars with the effective temperatures ranging from $T_{\rm eff} = 2\,000$ K to $T_{\rm eff} = 10\,000$ K and with the surface gravities ranging from $\log g = 0$ to $\log g = 8$. It must be noted that stellar gravities much higher than $\log g = 5$ are characteristic for white dwarfs, which have different internal structure than stars considered in this paper. As already discussed in Paper I the calculated wave energy fluxes for these stars there and in the present paper should not be directly compared to the wave energy fluxes specifically obtained for white dwarfs (see Böhm & Cassinelli 1971; Arcoragi & Fontaine 1980; Musielak 1987). We nevertheless included acoustic fluxes for high-gravity stars in our present work for comparison, to show the effect of metallicity (for details see Sect. 3).

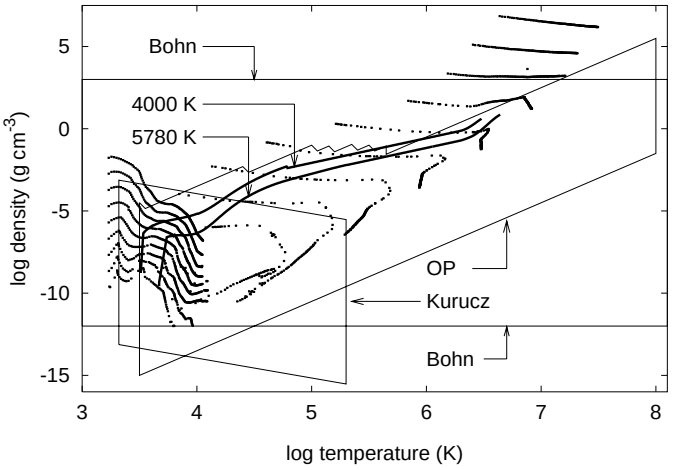

Fig. 1. Range of opacity tables in the $\log\rho$ vs. $T_{\rm eff}$ plane. The dots indicate the state at the outer (*left*) and inner (*right*) boundaries of stellar convection zone models. The solid lines show the full temperature and density dependence of two convection zone models with indicated $T_{\rm eff}$ and $\log g = 4.44$.

In the present paper, we have used tables from the opacity project OP (Seaton 1993, 1996; also Seaton et al. 1994) as well as opacities calculated with the ATLAS-program of Kurucz (1992, 1996). These tables are available for solar chemical abundance, i.e. abundance by mass of hydrogen $X_{\rm m} = 0.70$, helium $Y_{\rm m} = 0.28$ and of metals $Z_{\rm m} = 2 \cdot 10^{-2}$, as well as for reduced metallicity compared to the solar composition. The logarithm of the reduction factor is given in square brackets. We consider the following metal abundances: $Z_{\rm m} = 2 \cdot 10^{-2} \mathrel{\widehat{=}} [0]$, $Z_{\rm m} = 2 \cdot 10^{-3} \mathrel{\widehat{=}} [-1]$, $Z_{\rm m} = 2 \cdot 10^{-4} \mathrel{\widehat{=}} [-2]$, $Z_{\rm m} = 2 \cdot 10^{-5} \mathrel{\widehat{=}} [-3]$ and $Z_{\rm m} = 0 \mathrel{\widehat{=}} [-\infty]$. For comparison we have also employed the opacities (henceforth called 'Bohn'-opacities) used in our acoustic energy generation calculations of Paper I; these opacities are valid for solar abundances and were compiled by Bohn (1984) and Theurer (1993) from various opacity tables given by Alexander (1975, 1989), Cox & Tabor (1976), Yorke (1979, 1980), Meyer-Hofmeister (1982), and Weiss (1990).

Fig. 1 displays the ranges of validity (marked Bohn, OP, Kurucz) for the above mentioned opacity tables in a $\log\rho$ versus $\log T$ diagram. Note that the Bohn-opacities with their range $1 \le \log T \le 9$ occupy a rectangle and extend beyond the figure. The ranges of the OP- and Kurucz-opacities are the parallelogram-shaped regions. In addition, dots seen in Fig. 1 mark the outer and inner boundaries of the convection zone in our envelope models computed in the same way as described in Paper I. The nine closely packed dotted curves in the range $3.2 \le \log T \le 4$ represent (from the bottom to the top) the outer boundaries of the convection zones of our models for the nine gravities $\log g = 0, 1, \cdots 8$. For each $\log g$, the effective temperature $T_{\rm eff}$ increases from left to right in the range $2\,000 \le T_{\rm eff} \le 10\,000$ K. The nine dotted curves extending

from $\log T \approx 4$ to the right upper corner of Fig. 1 represent the inner boundaries of the convection zones of our models for the nine mentioned gravities (where the gravity again increases from the bottom to the top). With increasing $T_{\rm eff}$, the densities at the inner boundaries decrease similarly as for the outer boundaries. In Fig. 1, each convection zone is indicated by its inner and outer boundary point. These convection zone models are part of our complete envelope models which at the surface started with the photospheric radiative equilibrium model and extended somewhat below the convection zone. These radiative equilibrium photosphere models are not shown in Fig. 1 since for the sound generation we are only interested in the convection zones. However, for illustration, Fig. 1 also presents (solid lines) the dependence of ρ on T for two complete envelope models of main sequence stars with $T_{\rm eff} = 4000, 5780$ K and $\log g = 4.44$. For these models the line sections of nearly constant temperature near the outer boundary indicate the photospheric radiative equilibrium boundary layers.

Obviously for high temperatures and densities present in the deep stellar interior, some of the $(T,\ \rho)$ values taken for the stellar models exceed the ranges given by the OP- as well as by the Kurucz-opacities. As we are only interested in the stellar layers immediately below the photosphere rather than in the deep stellar interior, we continued the convection zone computation in the interior with the last entry of the opacity table before the range of the table was exceeded. This introduces negligible errors as the opacities above sufficiently high $(T,\ \rho)$ values are dominated by electron scattering where the opacity per gram is constant.

The above procedure cannot be applied at the outer boundary of the table (at small $(T,\ \rho)$), because the structure of the convection zone and the generated acoustic flux depends sensitively on these surface values. This is also the region where the changes in metal abundance have their biggest impact. For this reason we abort calculations of stellar convection zone models if they fall outside the lower $(T,\ \rho)$ boundary of the opacity table. However, we permit the initial pressure iteration of the radiative equilibrium surface layer to proceed when a boundary value of the κ-table is used. The limited range of the opacity tables presents a severe restriction to the range of models which we are able to compute. But even for the successfully computed models the uncertainty increases for stars with very low $T_{\rm eff}$. The results presented here remain preliminary, until the range of the opacity tables can be extended down to temperatures as low as 1 000 K.

3. Stellar acoustic fluxes and spectra

Keeping all these shortcomings in mind, we have calculated the acoustic wave energy fluxes and spectra for different stars in the Hertzsprung-Russell diagram (HRD) by using different mass fractions of metals $Z_{\rm m}$. As the tables of Kurucz include the microturbulent velocity $v_{\rm turb}$ as parameter, we follow Kurucz (1992) and take $v_{\rm turb} = 1$ km s^{-1} for all considered models. The OP-opacities are tabulated for reduction factors $[0]$, $[-1]$, $[-2]$ and $[-\infty]$. The tables by Kurucz for the lowest metallicity

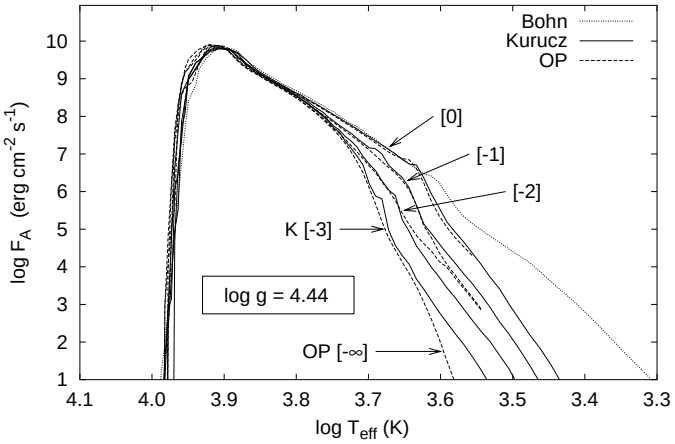

Fig. 2. Stellar acoustic fluxes, $F_{\rm A}$, are plotted versus the effective temperature, $T_{\rm eff}$, for stars with $\log g = 4.44$ and different metallicities $Z_{\rm m}$. The metallicities $\log Z_{\rm m}$ relative to solar are indicated in square brackets. The Bohn tables are valid for solar chemical composition, i.e. $Z_{\rm m} = 2 \cdot 10^{-2}$. As the OP tables are not given for $Z_{\rm m} = 2 \cdot 10^{-5}$, the table for $Z_{\rm m} = 0$ was used, labeled by $[-\infty]$.

are valid for reduction factors of $[-3]$. Although Seaton (1996) published codes for performing interpolations in $X_{\rm m}$ and $Z_{\rm m}$, we nevertheless take the OP-table with $Z_{\rm m} = 0$ for the lowest metallicity.

3.1. Dependence on T_{eff} and Z_m

Fig. 2 shows the calculated acoustic fluxes for main-sequence stars with $\log g = 4.44$. The presented results clearly demonstrate that the acoustic flux, $F_{\rm A}$, generated in stars with effective temperatures above $T_{\rm eff} \approx 6\,300$ K ($\log T_{\rm eff} = 3.8$), where neither the stellar structure nor the opacities are effected by the metal abundance, are independent of metallicity. Below this temperature, however, the generated acoustic flux for given $T_{\rm eff}$ strongly depends on the metallicity $Z_{\rm m}$. For models with the Kurucz-opacity and with $T_{\rm eff} = 4000$ K ($\log T_{\rm eff} = 3.6$) or lower, we find that the acoustic flux roughly decreases by a factor of ten when the metal abundance decreases by a factor of ten.

As seen in Fig. 2, there are also discrepancies between the acoustic fluxes calculated from models with different opacities. These discrepancies become especially prominent for stars with $T_{\rm eff} = 4000$ K ($\log T_{\rm eff} = 3.6$) and lower. Since the differences between the used opacity tables remain small even at low temperatures, we believe that the described discrepancies in $F_{\rm A}$ are caused by the limited range of these tables. Another possible source of these discrepancies is our use of the boundary values in the tables for the initial pressure iteration in the radiative equilibrium layer. Obvious exceptions are the calculated fluxes for the case of zero metallicity, $Z_{\rm m} = 0$, by using the OP-tables. For this case, the acoustic flux is considerably smaller than the values calculated with the Kurucz [-3] opacity table. Thus, we conclude that decreasing the metal abundance always reduces the resulting acoustic wave energy flux.

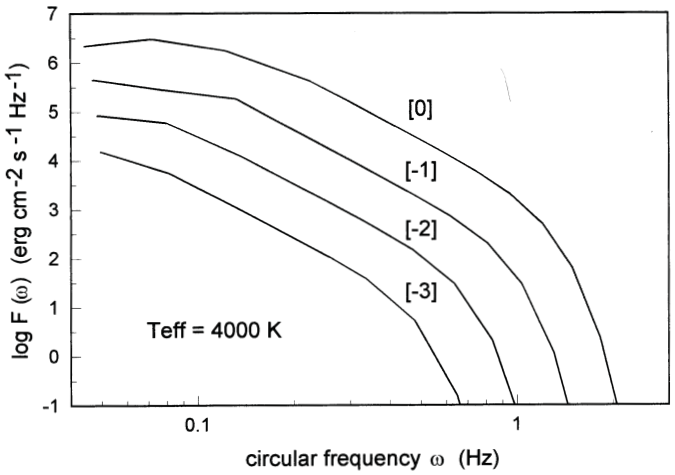

Fig. 3. Acoustic wave energy spectra, $F(\omega)$ (erg cm^{-2} s^{-1} Hz^{-1}) where ω is circular frequency, are plotted for stars with the effective temperature $T_{\rm eff}$ = 4000 K, $logg = 4.44$, and different metallicities. The presented results were obtained by using the Kurucz [0], [-1], [-2] and [-3] opacity tables.

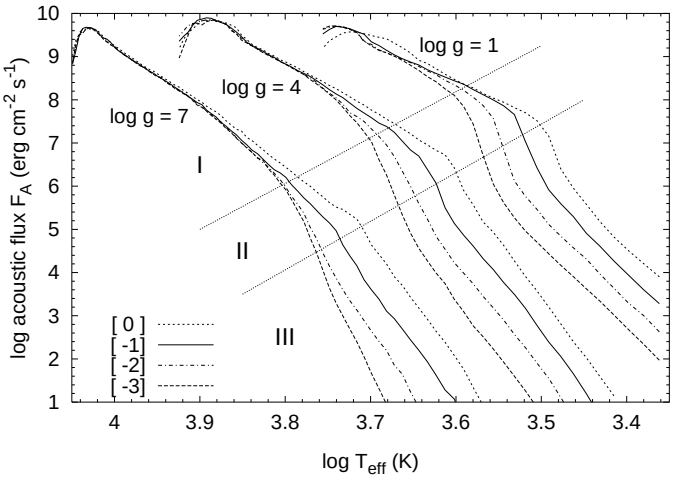

Fig. 5. Acoustic fluxes are plotted versus effective temperatures for different stellar gravities and metallicities. The results were obtained by using the Kurucz opacity tables. The domains I, II and III representing different dependence of the calculated fluxes on the metallicity are also shown.

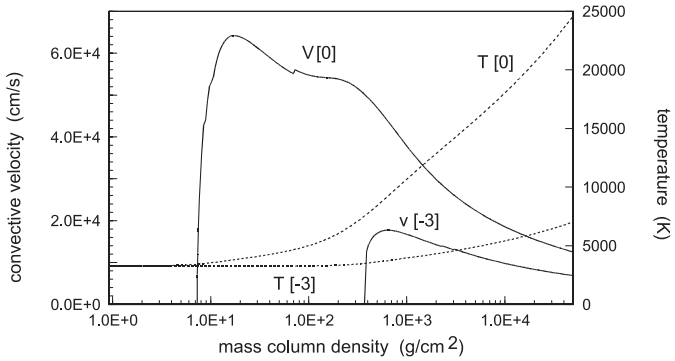

Fig. 4. Convective velocities and temperatures are plotted versus mass column density in the outermost layers of the convection zone for two stars with $T_{\rm eff} = 4\,000$ K and $\log g = 4.44$. The calculations were performed by using the Kurucz [0] and [-3] opacity tables.

Before the dependence of stellar acoustic fluxes on metallicity is further investigated for stars of different gravity (see Sect. 3.3), we want now to present typical wave energy spectra generated in stellar convection zones. Examples of these spectra for stars with $\log g = 4.44$, $T_{\rm eff} = 4000$ K, and different metallicity are shown in Fig. 3. It is seen that aside from a general decrease in the wave flux already presented in Fig. 2, the shape of the calculated acoustic wave energy spectrum does not depend on metallicity. A similar figure for stars with $T_{\rm eff} = 6000$ K shows essentially identical acoustic spectra to drafting accuracy. This indicates that shapes of stellar acoustic spectra presented in Paper I remain the same even if different values of metallicity are considered.

3.2. Dependence of convective velocities on metallicity

As already mentioned in Sect. 1, the efficiency of the generation of acoustic waves in stellar convection zones strongly depends on the structure of their outermost layers, where the convective velocities are largest. Typically, the upper boundary of stellar convection zone occurs approximately at a depth where the optical depth, τ, is unity; at this depth the opacity becomes so small that the rising convective bubbles can radiate their excess heat directly into space. For cool stars, lowering the metallicity decreases the opacity in such a way that $\tau = 1$ is located in deeper layers where the gas density is much higher. Thus, decreasing the metal content in these stars moves the top of their convection zones to deeper layers. The effect is shown in Fig. 4, which presents convective velocities and temperatures in the outermost convective layers of stars with $T_{\rm eff} = 4\,000$ K and $\log g = 4.44$. It is clearly seen that lowering the opacity from solar abundances $[0]$ to $[-3]$ moves the top of the convection zone (seen by the onset of convection) in this star from the mass column density $m = 7.0$ to $380\ g\,cm^{-2}$. This change in depth to higher mass column densities is due to the fact that the opacity in the $[0]$ star is about $1.5 \cdot 10^{-2}$ whereas for the $[-3]$ star it is $3 \cdot 10^{-4}\ cm^2\ g^{-1}$. Since for efficient convection the convective flux is roughly given by $\rho v_c^3 \approx \sigma T_{\rm eff}^4$ (Cox & Giuli 1968), the increase in density by a factor of 54 requires a convective velocity v_c to decrease by a factor of $(54)^{1/3} = 3.8$ (see Fig. 4). The large sensitivity of the acoustic flux generation to the value of the convective velocity explains then why for cool stars the lowering of the metal content strongly decreases the acoustic flux. On the other hand for hot stars, where hydrogen is primarily responsible for the stellar opacity, the upper boundary of stellar convection zones remain unchanged and, therefore, the resulting acoustic flux is not sensitive to any changes in metallicity.

3.3. Dependence on T_{eff}, $log\ g$ and Z_m

According to the results presented in Figs. 2 and 5, there are three domains (labeled I, II, III in Fig. 5) of different dependence of the acoustic flux on metallicity. These domains can be roughly

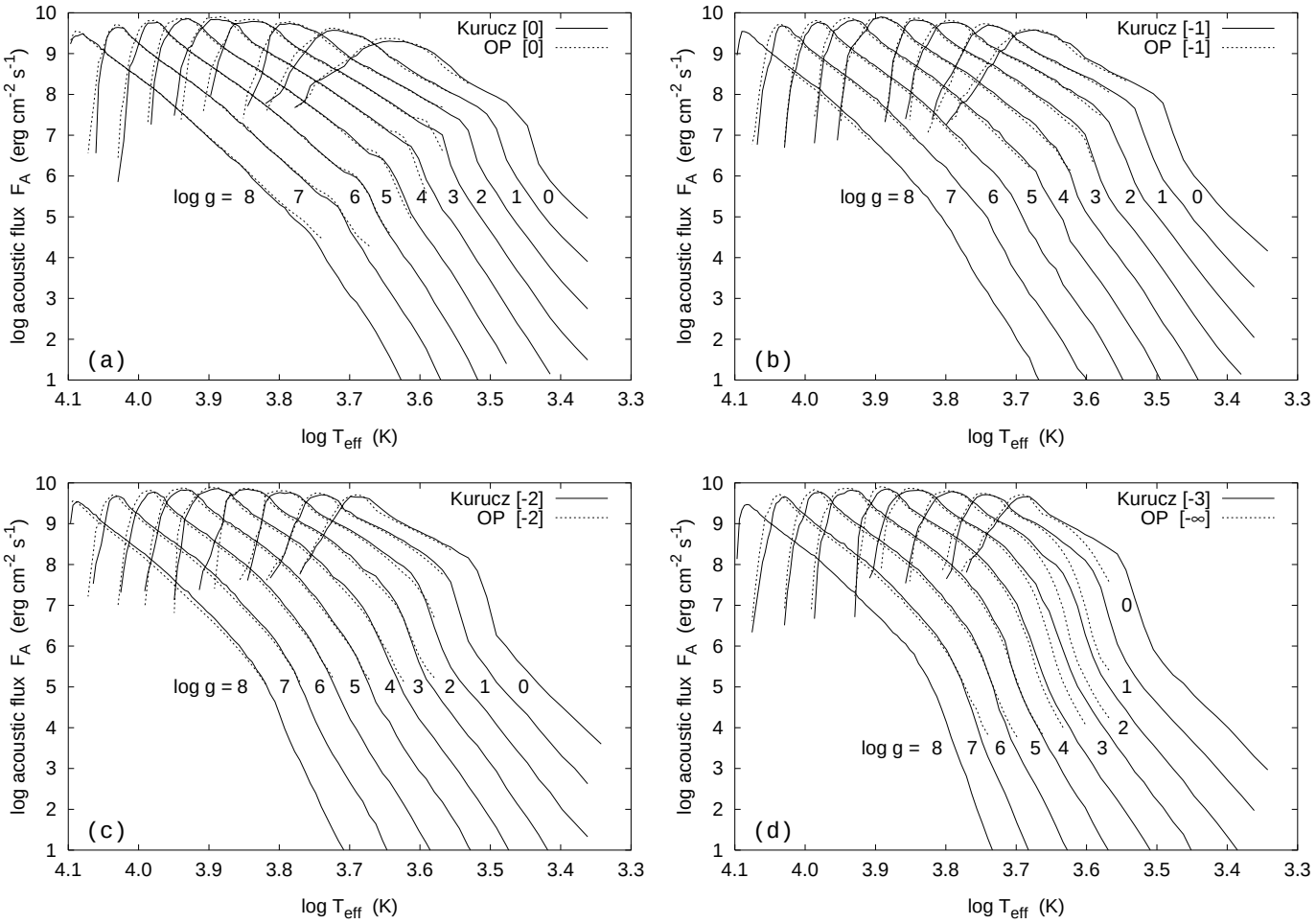

Fig. 6a–d. Acoustic fluxes for stars of different spectral and luminosity classes are plotted. The calculations were performed by using the Kurucz and OP opacity tables. The fluxes shown in panels **a** and **b** were obtained with $Z_{\rm m} = 2 \cdot 10^{-2}$ and $Z_{\rm m} = 2 \cdot 10^{-3}$, respectively. The fluxes in panel **c** were obtained with $Z_{\rm m} = 2 \cdot 10^{-4}$, and in panel **d** by using the Kurucz opacity tables with $Z_{\rm m} = 2 \cdot 10^{-5}$ and the OP opacity tables with $Z_{\rm m} = 0$

defined by two simple relations: $\log T_{\rm eff} = 28.4 \log g - 100$, which represents a dividing line separating domains I and II, and $\log T = 27.3 \log g - 95$, which represents a dividing line separating domains II and III.

Stars in domain I have $T_{\rm eff}$ high enough so that a significant fraction of hydrogen is ionized at the top of the convection zone. Hence, hydrogen is the main source of opacity and there is no or little dependence on the metal abundance $Z_{\rm m}$. In these stars the top boundary of their convection zone remains unchanged (in terms of mass column density) for different values of $Z_{\rm m}$, which implies that the maximum of the convective velocity is not sensitive to the metal content. As a result, the generated acoustic flux $F_{\rm A}$ does not depend on the stellar metallicity. It must be noted that at higher effective temperatures, convection ceases to exist and no acoustic flux is generated. Another problem that has to be addressed is the spatial extension of convection zones in stars that produce acoustic fluxes beyond the crest of the $F_{\rm A}$ curves (see Fig. 5). In these stars, the size of their convection zones falls below a pressure scale height H_p, which means that the fundamental assumption of the mixing length theory is no longer valid; according to this assumption a bubble due to buoyancy must travel at least a length $l = \alpha H_p$, where $\alpha = 2$, before it dissolves. In addition, large scattering of the calculated flux values occurs, so we smooth them by keeping always the largest fluxes and omitting the smaller ones. In summary, stellar acoustic fluxes shown in Fig. 5 beyond the crest of the $F_{\rm A}$ curves are not very reliable.

For stars of low $T_{\rm eff}$ in domain III, the outermost layers of their convection zones are strongly effected by the metal opacity (see Fig. 4 and discussion in Sect. 3.2). For these stars we find that lowering the metal abundance by a factor ten decreases the acoustic flux by roughly also a factor of ten. The effect becomes even more prominent for stars with higher gravity. The acoustic flux is about a factor of seven smaller for $\log g \approx 1$, if the metallicity is lowered by one order of magnitude, while for $\log g \approx 4$, $F_{\rm A}$ is about a factor of ten smaller.

In domain II of intermediate $T_{\rm eff}$ the transition between domains I and III occurs. Here $F_{\rm A}$ increases very rapidly with increasing $T_{\rm eff}$, an increasing fraction of hydrogen becomes ionized and affects the opacity.

Figs. 6 show the acoustic fluxes as a function of $T_{\rm eff}$ (with $\log g$ and the metallicity as parameters) for late-type stars. The fluxes were calculated by using both the Kurucz and the OP opacity tables. For the turbulent energy spectrum an extended Kolmogorov spatial spectrum with a modified Gaussian frequency factor (see Paper I) was taken and a mixing-length parameter $\alpha = 2.0$ was used in all calculations described in the present paper. Note that the fluxes obtained by using the OP opacity tables (see dotted lines in Figs. 6) are limited only to the domain I and II. This is caused by the fact that low effective temperatures of stars in the domain III are out of range of temperatures of the OP opacity tables. For the OP $[-\infty]$ calculations (Fig. 6d), $F_{\rm A}$ values are found to be considerably smaller than those obtained by using the Kurucz $[-3]$ opacity tables. It is very likely that the transition from $Z_{\rm m} = 2 \cdot 10^{-5}$ to $Z_{\rm m} = 0$ still has a noticeable effect on the acoustic flux.

Finally, it should be mentioned that our "grey" treatment of the radiative photospheric layers and the outermost layers in stellar convection zones is rather simplistic. Since the "non-grey" effects are expected to be especially important for cool late-type stars, and since for these stars also some opacities are missing, our results must be taken with some reservation for stars of very low $T_{\rm eff}$.

4. Conclusions

The acoustic wave energy fluxes and spectra have been computed for late-type stars of different spectral types, different luminosities and different metallicities (population I and II stars) by using Bohn's stellar envelope code described in Paper I, and the Kurucz and OP opacity tables. The main obtained results can be summarized as follows:

1. The Hertzsprung-Russel diagram can be subdivided into three domains (labeled I, II and III) representing a different dependence of the generated acoustic fluxes on the stellar metal abundance.
2. In domain I, stars have high enough $T_{\rm eff}$ so that the opacity is mainly due to hydrogen and is largely independent of the metal content. Likewise the acoustic flux arising from the narrow region near the maximum of the convective velocity is essentially independent of the stellar metal content.
3. In domain III, stars have low enough $T_{\rm eff}$ so that the metallicity strongly influences the opacity in the stellar surface layers. As a result, the generated acoustic fluxes decrease roughly by an order of magnitude for every order of magnitude decrease of the metal content.
4. The domain II signifies the transition between domains I and III. In this domain, the generated acoustic fluxes depend strongly on $T_{\rm eff}$.
5. The boundaries between the domains I and II, and II and III, have been defined by simple relationships between stellar effective temperatures and gravities.

Acknowledgements. We are grateful to Deutsche Forschungsgemeinschaft and NATO for support of this research. The work was also partially funded by NSF (grant number ATM-9526196) and by the NASA Astrophysics Theory Program (grant number NAG5-3027) to the University of Alabama in Huntsville. Z.E.M. also acknowledges support of this work by the Alexander von Humboldt Foundation.

References

Alexander D.R., 1975, ApJS 29, 363
Alexander D.R., 1989, ApJ 345, 1014
Arcoragi J.P., Fontaine G., 1980, ApJ 242, 1208
Böhm H.U., Cassinelli J., 1971, A&A 12, 21
Bohn H.U., 1984, A&A 136, 338
Cox A.N., Giuli T.R., 1968, Stellar Structure. Gordon and Breach, New York
Cox A.N., Tabor J.E., 1976, ApJS 31, 271
Goldstein M.E., 1976, Aeroacoustics. McGraw Hill, New York, p. 94
Kurucz R.L., 1992, In: Barbuy B., Renzini A. (eds.) IAU Symp. 149, The stellar population of galaxies. Kluwer, Dordrecht
Kurucz R.L., 1996, In: Adelman S.J., Kupka F., Weiss W. (eds), Workshop on model atmospheres and spectrum synthesis. ASP Conference Series 108
Lighthill M.J., 1952, Proc. Roy. Soc. A 211, 564
Meyer-Hofmeister E., 1982, Stellar Structure and Evolution. In: Schaifers K., Voigt H.H. (eds.), Landolt-Börnstein, Neue Serie VI, Vol.2b, Sect. 4.4.2.3.1., Springer, Berlin
Musielak Z.E., 1987, ApJ 322, 234
Musielak Z.E., Rosner R., Stein R.F., Ulmschneider P., 1994, ApJ 423, 474
Proudman I., 1952, Proc. Roy. Soc. A 214, 119
Seaton M.J., 1993, MNRAS 265, L25
Seaton M.J., 1996, MNRAS 279, 95
Seaton M.J., Yan Y., Mihalas D., Pradhan A.K., 1994, MNRAS 266, 805
Stein R.F., 1967, Solar Physics 2, 385
Theurer J., 1993, Dipl. Thesis, University of Heidelberg
Theurer J., Ulmschneider P., Musielak Z.E., 1996, In: Pallavicini R., Dupree A. (eds.) Cool Stars, Stellar Systems and the Sun. ASP Conf. Ser. 109, p. 169
Ulmschneider P., Theurer J., Musielak Z.E., 1996, A&A 315, 212
Weiss A., 1990, At. Data Nucl. Data Tables 45, No. 2, 209
Yorke H.W., 1979, A&A 80, 308
Yorke H.W., 1980, A&A 85, 215